Direct measurement of the recovery time of superconducting nanowire single-photon detectors

Claire Autebert, Gaëtan Gras (iD), Emna Amri, Matthieu Perrenoud (iD), Misael Caloz, Hugo Zbinden, and Félix Bussières

View Online   Export Citation   CrossMark

ARTICLES YOU MAY BE INTERESTED IN

Lithium-niobate-on-insulator waveguide-integrated superconducting nanowire single-photon detectors
Applied Physics Letters **116**, 151102 (2020); https://doi.org/10.1063/1.5142852

NbTiN thin films for superconducting photon detectors on photonic and two-dimensional materials
Applied Physics Letters **116**, 171101 (2020); https://doi.org/10.1063/1.5143986

Amorphous superconducting nanowire single-photon detectors integrated with nanophotonic waveguides
APL Photonics **5**, 076106 (2020); https://doi.org/10.1063/5.0004677

Direct measurement of the recovery time of superconducting nanowire single-photon detectors

Claire Autebert,[1] Gaëtan Gras,[1,2,a)] (iD) Emna Amri,[1,2] Matthieu Perrenoud,[1] (iD) Misael Caloz,[1] Hugo Zbinden,[1] and Félix Bussières[1,2]

AFFILIATIONS

[1] Group of Applied Physics, University of Geneva, CH-1211 Geneva, Switzerland
[2] ID Quantique SA, CH-1227 Carouge, Switzerland

[a)] Author to whom correspondence should be addressed: gaetan.gras@idquantique.com

ABSTRACT

One of the key properties of single-photon detectors is their recovery time, i.e., the time required for the detector to recover its nominal efficiency. In the case of superconducting nanowire single-photon detectors (SNSPDs), which can feature extremely short recovery times in free-running mode, a precise characterization of this recovery time and its time dynamics is essential for many quantum optics or quantum communication experiments. We introduce a fast and simple method to characterize precisely the recovery time of SNSPDs. It provides full information about the recovery of the efficiency in time for a single or several consecutive detections. We also show how the method can be used to gain insight into the behavior of the bias current inside the nanowire after a detection, which allows predicting the behavior of the detector and its efficiency in any practical experiment using these detectors.

Published under license by AIP Publishing. https://doi.org/10.1063/5.0007976

I. INTRODUCTION

Single-photon detectors are a key component for optical quantum information processing. Among the different technologies developed for single-photon detection, superconducting nanowire single-photon detectors (SNSPDs) have become the first choice of many applications showing performance orders of magnitude better than their competitors. These nano-devices have stood out as highly promising detectors thanks to their high detection efficiency,[1] low dark count rate,[2] excellent time resolution,[3,4] and fast recovery.[5] SNSPDs have already had an important impact on demanding quantum optics applications such as long-distance quantum key distribution,[6] quantum networking,[7] optical quantum computing,[8] device-independent quantum information processing,[9,10] and deep space optical communication.[11]

Depending on the application, some metrics become more important than others and can require extensive characterization. One example is the quantum key distribution (QKD), where the recovery time of SNSPDs limits the maximum rate at which it can be performed. In such a case, studying the time evolution of the SNSPD efficiency after a detection becomes important and would give us insight into the detector's behavior, allowing the prediction of experimental performances. Obtaining accurate information is, however, a non-trivial task because the recovery time is intrinsically linked to the time dynamics of the bias current flowing inside the detector.

There are several methods used to characterize the recovery time of the efficiency of a SNSPD. The first one uses the output pulse delivered by the readout circuit to gain knowledge about the recovery time dynamics. However, we cannot fully trust this method since the time decay of the output voltage pulse is inevitably affected by the amplifier's bandwidth and by all other filtering and parasitic passive components. In the best case, we can only have an indirect estimation of the efficiency temporal evolution. A second method might consist of extracting the recovery time behavior from the measurement of the detection rate as a function of the incident photon rate. This method can be performed with either a continuous-wave or a pulsed laser source. The main problem with the pulsed source configuration is that we can only probe the efficiency at time stamps multiple of the pulse period, which does not give full information about the continuous time dynamics.

Both methods have the drawback of only providing an average efficiency per arriving photon. They can moreover be very sensitive to external parameters such as the discriminator's threshold level. Hence, using one of these measurements does not allow one to make unambiguous predictions about the behavior of the detectors in other experiments. Another method is based on measuring the autocorrelation in time between two subsequent detections when the detector is illuminated with a continuous-wave laser[12] or a pulsed laser.[13] This method has the clear advantage over all other methods of allowing a direct observation of the recovery of the efficiency in time, and it can, therefore, reveal additional details (for example, the presence of afterpulsing). While the implementation of this autocorrelation method is relatively simple, the acquisition time can, however, be very long.

In this article, we introduce and demonstrate a novel method, simple in both its implementation and analysis, to fully characterize the recovery time dynamics of SNSPDs. This method is an improvement of the autocorrelation method mentioned above[13] and is similar to how the detector deadtime is observed in LIDAR experiments.[14,15] It has the advantage of a much shorter acquisition time with no need of data post-processing. We apply it to characterize the recovery time of SNSPDs under different operating conditions and for different wavelengths. We can also use it to estimate the variation of the current inside the detector after a detection and, consequently, gain insight into what happens to the bias current when two detections occur within the time period needed by the efficiency to fully recover. This method also allows us to reveal details that are otherwise difficult to observe, such as afterpulsing or oscillations in the bias current's recovery as well as predict the outcome of the count rate measurement.

II. HYBRID-AUTOCORRELATION METHOD

To investigate the time-dependence of the detection efficiency after a first detection event, a useful tool is the normalized time autocorrelation $G(\Delta t)$ defined by

$$G(\Delta t) = \frac{\langle n(t)n(t + \Delta t) \rangle}{\langle n(t) \rangle^2}, \tag{1}$$

where $n(t)$ is the number of detections at time t and $\langle . \rangle$ the temporal average. This value is proportional to the probability of having two detections separated in time by Δt.[16] For an ideal detector with a zero recovery time, the detection events occurring at times t and $t + \Delta t$ are independent when illuminated with coherent light. In this case, the autocorrelation will be equal to one for any value of Δt. For a detector with a non-zero recovery time, the autocorrelation function will be equal to zero at $\Delta t = 0$, and then it will recover toward one with a shape that is directly indicative of the value of the efficiency after a detection occurring at time zero.

This method can be implemented with a continuous-wave (CW)[12] or a pulsed laser,[13] and it has the advantage of allowing a direct observation of the recovery of the efficiency in time. Its implementation requires a statistical analysis of the inter-arrival time between subsequent detections. A schematic of an implementation of this method with a pulsed laser is shown in Fig. 1(a), and we use it for comparison with the novel method we introduce hereafter. A delay generator (DG) is used to generate two laser pulses with a controllable time delay between them. The triggerable laser is generating short pulses that are then attenuated down to ≈ 0.1 photon per pulse by calibrated variable attenuators. The output signal of the detector is fed to a time-to-digital converter (TDC) that records the arrival times of the detections.

To reconstruct the recovery of the efficiency in time after a first detection, we analyze the time stamps to estimate the probability of the second detection as a function of its delay with respect to the first one. This method can be significantly time consuming because only one given delay can be tested at once. Moreover, one needs a detection to occur in the first pulse to count the occurrences. It also requires to have the same power in both pulses, and this power needs to be very stable during the whole duration of the
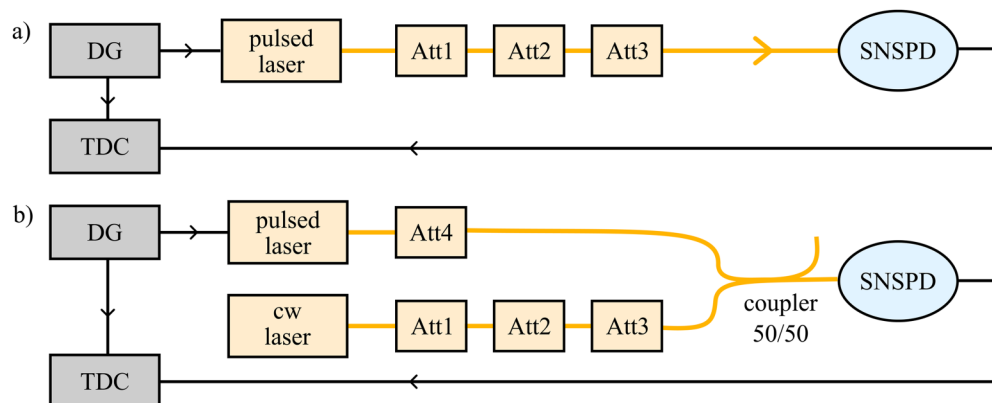

FIG. 1. Schematics of the experimental setups for the (a) pulsed-autocorrelation method and for the (b) hybrid-autocorrelation method. DG, delay generator; TDC, time-to-digital convertor; Att, attenuators.

experiment, which can be difficult to guarantee with some triggered lasers such as gain-switched laser diodes.

Here, we introduce a new method, named *hybrid-autocorrelation*, that combines the pulsed and CW autocorrelation methods. The advantages of this hybrid measurement are its rapidity, flexibility in terms of wavelengths, ability to faithfully reveal the shape of the recovery of the efficiency as well as tiny features such as optical reflections in the system or even oscillations of the bias current after the detection, and most importantly, it does not require any post-processing to extract information. In the hybrid-autocorrelation method [Fig. 1(b)], a light pulse containing a few tens of photons is used to make the detector click with certainty at a predetermined time, which greatly reduces the total collection time needed to build the statistics. This pulse is combined on a beam splitter with a weak but steady stream of photons (typically about 10^6 photons/second or less) coming from an attenuated CW laser. These photons are used to induce a second detection after the one triggered by the pulsed laser, and the detection probability is proportional to the efficiency at this given time. To record the detection times, we use a TDC building start–stop histogram configuration, where the start is given by the DG triggering the pulsed laser.

III. RESULTS

We implemented the pulsed and hybrid-autocorrelation methods using a gain-switched pulsed laser diode at either 980 nm with a 300 ps pulse width or 1550 nm with a 33 ps pulse width and a tunable CW laser (for the hybrid method). We used meandered and fiber-coupled molybdenum silicide (MoSi) SNSPDs fabricated by the University of Geneva[4] and cooled at 0.87 K. We tested five devices referred as A, B, C, D, and E. These devices have a nanowire width of 110 nm–150 nm, a fill factor of 0.5–0.6, and an active area diameter ranging from 9 to 16 μm. The arrival times of the detections was recorded with a TDC (ID900 from IDQ) with
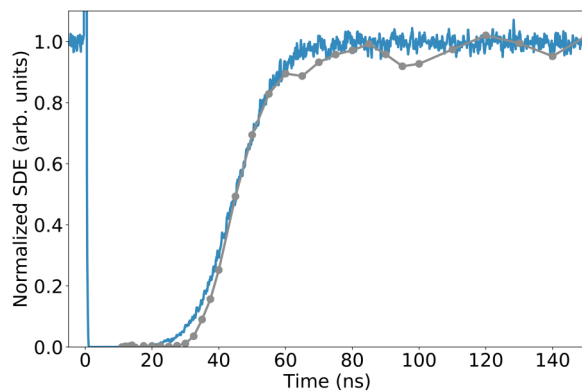
FIG. 2. Normalized system detection efficiency (SDE) at 1550 nm as a function of the time delay between two events for the pulsed-autocorrelation method (gray points) and the hybrid-autocorrelation method (dark blue curve). For the hybrid-autocorrelation method, we renormalize the probability of detection for the photon coming from the CW laser. The pulsed laser triggering the detector each round at $t = 0$ ns will then give a value greater than one.

100 ps-wide time bins. Figure. 2 shows the temporal evolution of the normalized efficiency after a first detection obtained with the pulsed and hybrid-autocorrelation methods. The detector was biased very closely to the switching current I_{SW}, defined as the current at which the dark counts start to rise quickly. Both methods yielded similar results in the trend of the curves, but the pulsed-autocorrelation method gave a much larger scatter in the data. This scatter is caused by the instability of the laser power over the duration of the measurement (about 6 h). The hybrid-autocorrelation method measurement required only about 1 min of acquisition time with the pulsed laser triggering detections at a frequency of 1 MHz and gave the exact shape of the recovery of the efficiency. We also noticed that the detector does not show any afterpulsing effects; otherwise, the normalized efficiency curve could momentarily reach values larger than one.

A. Current inside the SNSPD after detection

The SNSPD is biased with a current I_b provided by a current generator through a bias tee. The detector can be at first order modeled by an inductance L_k representing the kinetic inductance of the nanowire, serially connected to a variable resistor whose value is 0, while the nanowire is superconductive. When a photon is absorbed and breaks the superconductivity, it creates a local resistive region called "hotspot" with a resistance $R_{hs} \sim 1 \, k\Omega$.[17] The current is then deviated to the readout circuit with a time constant $\sim L_k/R_{hs} \sim 1$ ns. Once the current has been shunted, the nanowire cools down and returns to thermal equilibrium allowing the current to return to the nanowire with a time constant of $\tau = L_k/R_L$, where $R_L = 50 \, \Omega$ is the typical load resistance [see Fig. 3(a)]. Note that, in practice, there may be other series resistance of a few ohms due to the coaxial cables connecting the SNSPD to the amplifier, which might slightly increase the effective value of R_L and, therefore, slightly decrease the value of τ. Also, the amplifiers are typically capacitively coupled, which is not shown here on the drawing. The drop and the recovery of the efficiency of the SNSPD after a detection are, therefore, directly linked to the variation of the current and to the relation between the detection efficiency and the bias current. In Fig. 3(b), we plot the system detection efficiency as a function of the bias current of a given MoSi SNSPD, and we observe that it follows a sigmoid shape.[18] We can, therefore, fit that curve using the equation

$$\eta = \frac{\eta_{max}}{2}\left[1 + \mathrm{erf}\left(\frac{I - I_0}{\Delta I}\right)\right], \tag{2}$$

where I_0 and ΔI are parameters for the sigmoid and η_{max} is the maximum efficiency of the detector. After a detection, the equivalent circuit of Fig. 3(a) indicates that the current variation after a detection should be described by
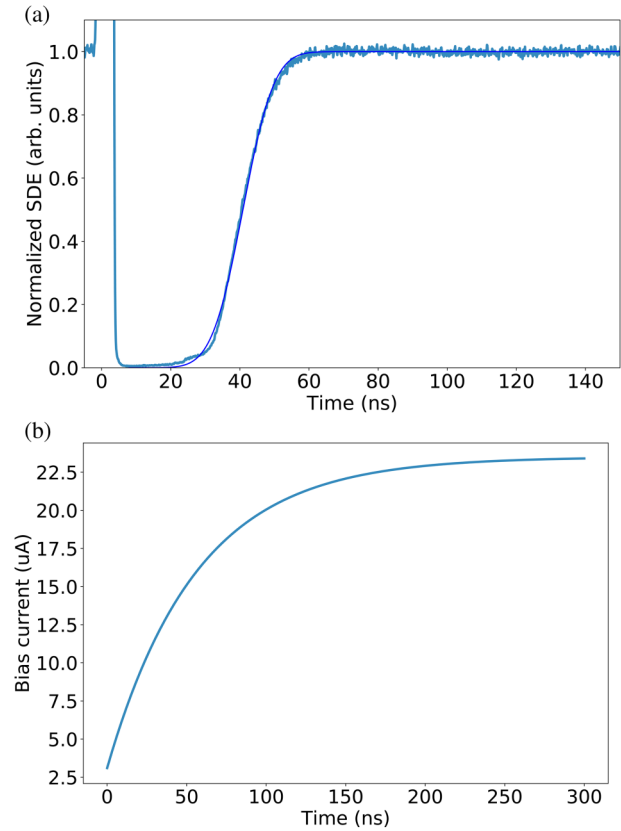
$$I = (I_b - I_{drop})\left(1 - \exp\left(-\frac{t}{\tau}\right)\right) + I_{drop}, \tag{3}$$

where I_b is the nominal bias current of operation of the detector just before a detection, I_{drop} is the current left in the nanowire immediately after a detection, and τ is the time constant for the
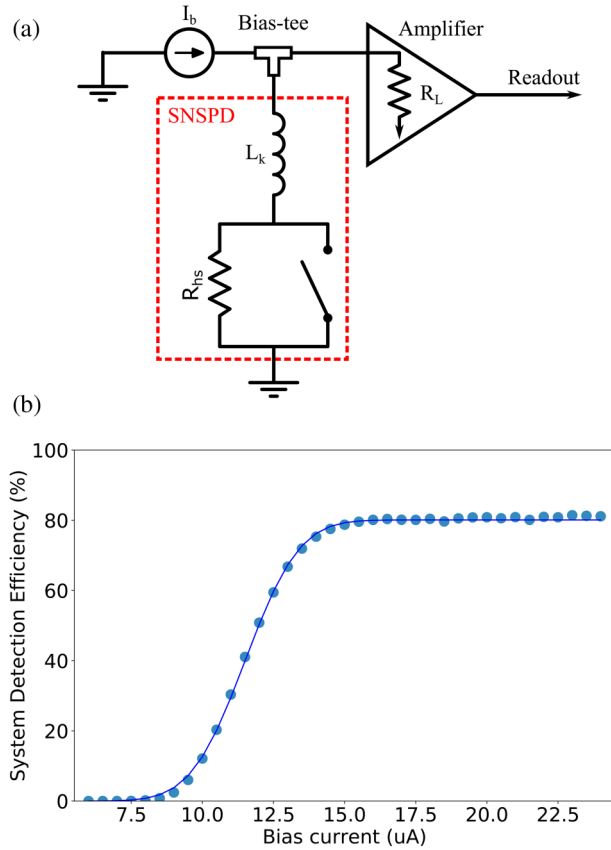
FIG. 3. (a) Simple equivalent electrical circuit of the detector and readout. We used a custom-made bias tee. The amplification is done in two steps: first with a cryogenic amplifier at 40 K and then with a ZFL500LN+ mini-circuit amplifier at room temperature. (b) Relation between the SDE at 850 nm and a bias current of device B.

FIG. 4. (a) Normalized efficiency at 850 nm of device B as a function of time after a first detection. The initial detection was triggered with a pulsed laser at 980 nm. (b) Reconstructed bias current of the detector as a function of time after the first detection.

return of the current. Here, we neglect the time formation of the hotspot (and, therefore, the time for I to go from I_b to I_{drop}) as, according to the electro-thermal model of Ref. 17, its lifetime is expected to be short (typically a few hundreds of ps) compared to the recovery of the current τ. By fitting the curve of the efficiency vs the current with Eq. (2) [Fig. 3(b)], we can infer I_0 and ΔI; by inserting Eq. (3) in Eq. (2) and fitting the recovery time measurement [Fig. 4(a)], we can estimate I_{drop} and τ. Here, we used $I_b = 23.5\,\mu A$, and the best fit is obtained with $I_{drop} = 0\,\mu A$ and $\tau = 60$ ns. Then, using both results, we can infer the value of the current in the nanowire vs time as shown in Fig. 4(b). It is worth noting that this method predicts that $I_{drop} > 0$ for several of the detectors we tested. Physically, this would mean that the current did not have time to completely leave the SNSPD before it became superconductive again. This is the kind of detail that is very difficult to measure directly. Admittedly, this prediction made with our method is not direct and, therefore, difficult to fully confirm. Moreover, with the values obtained for I_{drop} and τ, thanks to Eqs. (2) and (3) and the efficiency vs bias current and
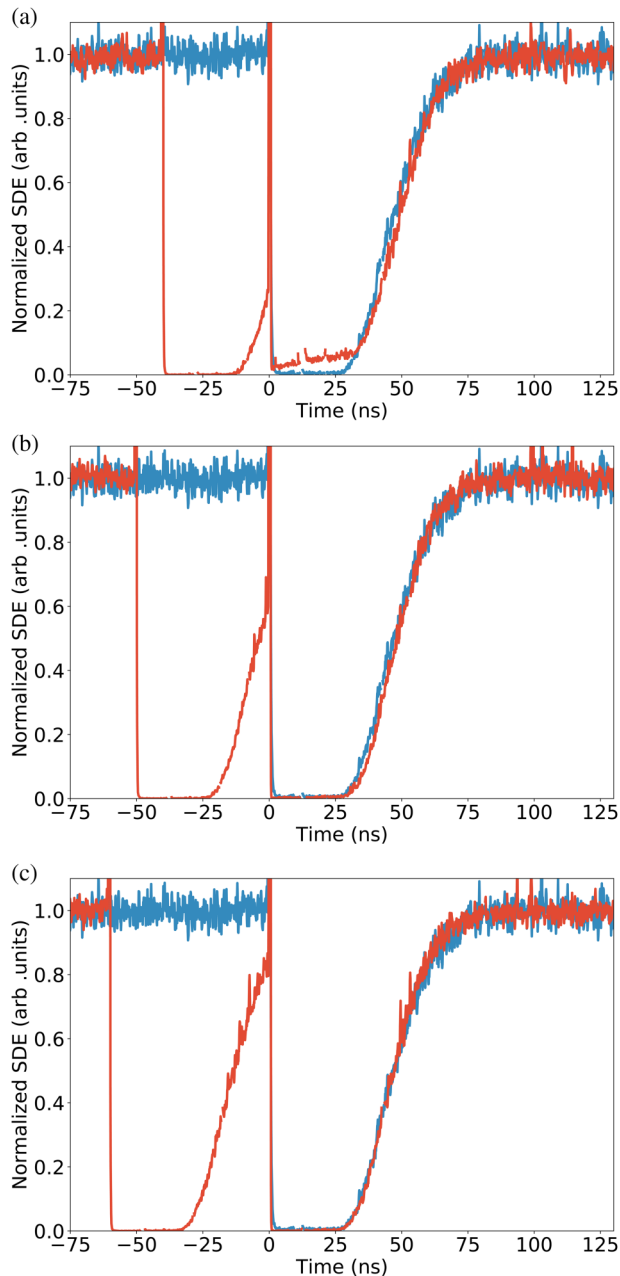
time recovery measurements, it is possible to accurately predict the behavior of a detector at high detection rates, as shown in Sec. III C. This gives us an increased confidence in the method proposed here.

When a photon strikes the nanowire and a detection occurs, the current inside the detector drops to a percentage of its original value and not necessarily to zero. An interesting measurement possible with our method consists of sending a train of pulses (here two) with varying delay between them to measure the efficiency recovery after the second detection. With several consecutive detections, we might expect some cumulative effect with the current dropping to lower and lower values. This would lead to a longer recovery time of the detector. The results of this measurement are shown in Fig. 5. The red curves correspond to the cases where two strong pulses were sent, with different time delays between them, and the blue curves correspond to the cases where only one strong pulse was sent. We can see that the shape of the autocorrelation curve for the third detection (in the case of two pulses) matches the one for the second detection (in the case of one pulse). The only difference observable comes from the 40 ns case where we get

some detection after the second trigger pulse. One possible explanation would be that some trigger pulses are not detected as the efficiency recovers less after a delay of 40 ns. This gives us good confidence that the current drops always to the same value. This has never been observed as clearly before despite being important
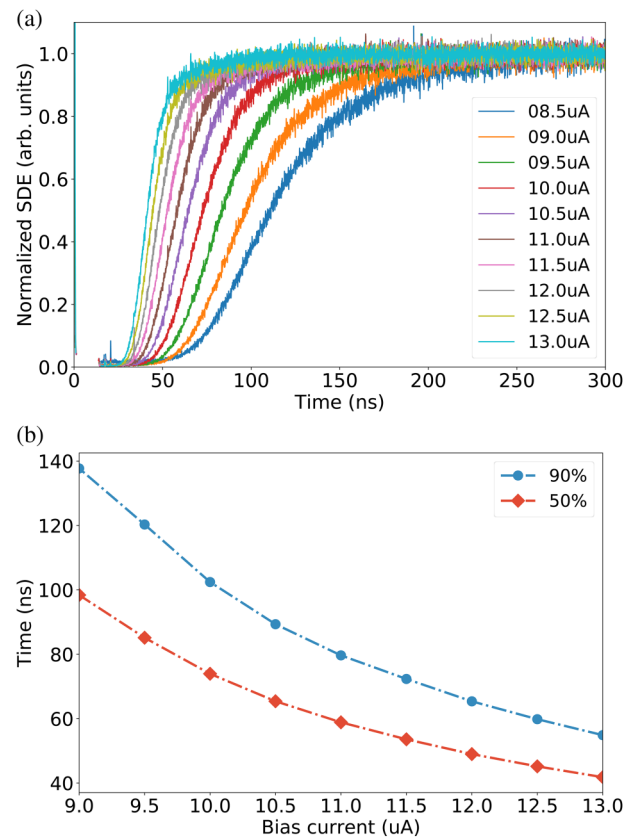
for performance characterization at high count rates. Indeed for experiment where the photons arrive with very short delays between them, it is important to know that the recovery time after any detection is the same and is not affected by the time delay between detections.

B. Current and wavelength dependency

Using the hybrid-autocorrelation method, we could also investigate the dependency of the recovery time on different operating conditions. First, we looked at the behavior with different bias currents. Figure 6(a) shows the time recovery histograms for different bias currents from $8.5\,\mu A$ to $13.0\,\mu A$, which correspond to the switching current I_{SW} of our detector. Figure 6(b) shows the time needed by the detector to recover 50% (red curve) and 90% (blue curve) of its maximum efficiency as a function of the bias current. The results show that the SNSPD recovery time is shorter for increasing bias current, which is expected from the shape of the efficiency curve with respect to the bias current [Fig. 3(b)]. Indeed, this curve exhibits a plateau, allowing the current that is re-flowing

FIG. 5. Recovery of the normalized SDE at 1550 nm of device C for one trigger pulse (blue curve) and for two trigger pulses (red curve) at 1550 nm with different delays between the pulses: (a) 40 ns, (b) 50 ns, and (c) 60 ns.

FIG. 6. (a) Recovery of the normalized SDE at 1550 nm for device D at different bias currents and (b) shows the time to recover 50% (red diamonds) and 90% (blue dots) of the maximum efficiency as a function of the bias current.
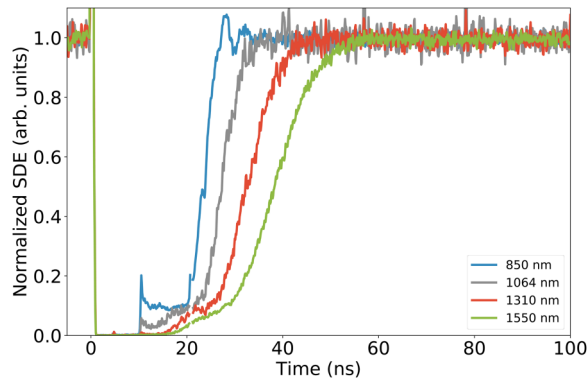
FIG. 7. Recovery of the normalized SDE of device E at different wavelengths. The initial detection was triggered with the 1550 nm pulsed laser.

FIG. 8. Count rate of device D with a continuous-wave laser: the red dots correspond to the count rate measurement vs the incident photon rate, and the blue curve corresponds to the prediction from the hybrid-autocorrelation measurement.

into the nanowire after a first detection, to reach the full efficiency faster.

Second, we vary the wavelength of the CW laser. Note that we do not need to change the wavelength of the pulsed laser because it does not influence the recovery time dynamics. It does influence the dynamic of the hotspot formation and disappearance,[17,19,20] but this happens over a time that is typically much smaller than 1 ns. We can see in Fig. 7 that the lower the wavelength, the faster the recovery time. With decreasing wavelength, the current needed to reach maximum efficiency is reduced, while the switching current stays unchanged. As the current dynamic in the nanowire is the same for all wavelengths, the detector recovers, therefore, its full efficiency quicker for a smaller wavelength. Interestingly, the curve at 850 nm seems to reveal some small oscillations of the efficiency around 30 ns after the trigger detection. While the origin of this small oscillation is not entirely clear (and we did not investigate this further), it nevertheless illustrates the capacity of the method to reveal some specific transient details of the efficiency recovery dynamics or of the interplay between the voltage pulse and the discrimination circuitry.

C. Predicting the counting rate with a continuous-wave source

We illustrate the predictive power of the hybrid-autocorrelation method proposed here by looking at the behavior of SNSPDs at a high counting rate, when the average time between two detections becomes comparable to the recovery time of the SNSPD. We model an experiment where the light of a continuous-wave laser is sent to the detector and the detection rate is measured as a function of the incident photon rate. To estimate the count rate vs the incident photon rate from the hybrid-autocorrelation method, we run a Monte-Carlo simulation. We randomly select the time t of arrival of the photon since the last detection using the exponential distribution (which gives the probability distribution of time intervals between events in a Poissonian process). Thanks to the autocorrelation measurement, we know the probability of a successful event (i.e., a detection) at time t. In the case of an
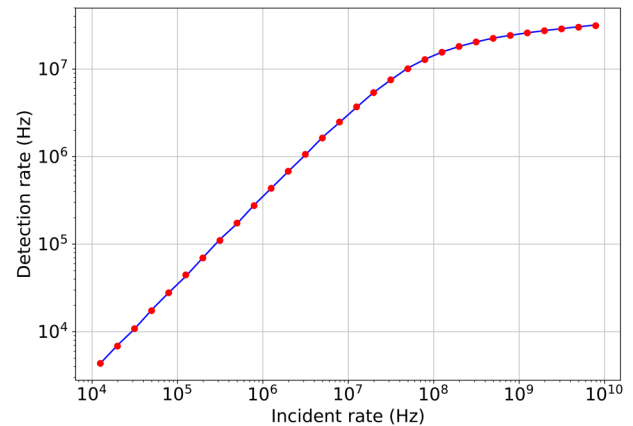
unsuccessful event, we look at the time $t + t'$ of arrival of the next photon. Once we have a detection, we start over. We run this until we have $N = 10\,000$ detections to estimate the count rate of the detector.

Figure 8 shows, for device D, the comparison between the experimental detection rate vs the incident photon rate of the SNSPD and its prediction from the hybrid-autocorrelation measurement. We can see that the count rate data and the count rate predicted from the autocorrelation measurement that gave us $I_{drop} = 2.9\,\mu A$ and $\tau = 58$ ns match very well together, giving a high trust in the model and in the predictive power of the method.

IV. CONCLUSION

The method we proposed here provides a fast, simple, and most importantly direct characterization of the recovery of the efficiency of a SNSPD detector. The measurements showed that the recovery of a SNSPD is faster with larger bias current and shorter wavelengths. We demonstrated that the current through a given detector always drops to the same non-zero value after detection even when subjected to several consecutive pulses all arriving within a fraction of the total recovery time of the SNSPD. We also showed that our method can be used to correctly predict how the detection rate of an SNSPD behaves when it becomes impeded by its recovery time. Therefore, we trust our method to allow predicting the behavior of the SNSPD in other experiments where the variation of the efficiency in time is of importance. Finally, it is also worth noting that this method can be applied to any type of a single-photon detector and could be considered as a universal benchmarking method to measure and compare the recovery time of single-photon detectors.

AUTHORS' CONTRIBUTIONS

C.A. and G.G. contributed equally to this work.

DATA AVAILABILITY

The data that support the findings of this study are available from the corresponding author upon reasonable request.

REFERENCES

[1]F. Marsili, V. B. Verma, J. A. Stern, S. Harrington, A. E. Lita, T. Gerrits, I. Vayshenker, B. Baek, M. D. Shaw, R. P. Mirin, and S. W. Nam, "Detecting single infrared photons with 93% system efficiency," Nat. Photonics. **7**, 210–214 (2013).

[2]H. Shibata, K. Shimizu, H. Takesue, and Y. Tokura, "Ultimate low system dark-count rate for superconducting nanowire single-photon detector," Opt. Lett. **40**, 3428–3431 (2015).

[3]B. A. Korzh, Q. Y. Zhao, S. Frasca, J. P. Allmaras, T. M. Autry, E. A. Bersin, M. Colangelo, G. M. Crouch, A. E. Dane, T. Gerrits, F. Marsili, G. Moody, E. Ramirez, J. D. Rezac, M. J. Stevens, E. E. Wollman, D. Zhu, P. D. Hale, K. L. Silverman, R. P. Mirin, S. W. Nam, M. D. Shaw, and K. K. Berggren, "Demonstrating sub-3 ps temporal resolution in a superconducting nanowire single-photon detector," arXiv:1804.06839 (2018).

[4]M. Caloz, M. Perrenoud, C. Autebert, B. Korzh, M. Weiss, C. Schönenberger, R. J. Warburton, H. Zbinden, and F. Bussières, "High-detection efficiency and low-timing jitter with amorphous superconducting nanowire single-photon detectors," Appl. Phys. Lett. **112**, 061103 (2018).

[5]A. Vetter, S. Ferrari, P. Rath, R. Alaee, O. Kahl, V. Kovalyuk, S. Diewald, G. N. Goltsman, A. Korneev, C. Rockstuhl, and W. H. P. Pernice, "Cavity-enhanced and ultrafast superconducting single-photon detectors," Nano Lett. **16**, 7085–7092 (2016).

[6]A. Boaron, G. Boso, D. Rusca, C. Vulliez, C. Autebert, M. Caloz, M. Perrenoud, G. Gras, F. Bussières, M.-J. Li, D. Nolan, A. Martin, and H. Zbinden, "Secure quantum key distribution over 421 km of optical fiber," Phys. Rev. Lett. **121**, 190502 (2018).

[7]F. Bussières, C. Clausen, A. Tiranov, B. Korzh, V. B. Verma, S. W. Nam, F. Marsili, A. Ferrier, P. Goldner, H. Herrmann, C. Silberhorn, W. Sohler, M. Afzelius, and N. Gisin, "Quantum teleportation from a telecom-wavelength photon to a solid-state quantum memory," Nat. Photonics. **8**, 775 (2014).

[8]X. Qiang, X. Zhou, J. Wang, C. M. Wilkes, T. Loke, S. O'Gara, L. Kling, G. D. Marshall, R. Santagati, T. C. Ralph, J. B. Wang, J. L. O'Brien, M. G. Thompson, and J. C. F. Matthews, "Large-scale silicon quantum photonics implementing arbitrary two-qubit processing," Nat. Photonics. **12**, 534 (2018).

[9]L. K. Shalm, E. Meyer-Scott, B. G. Christensen, P. Bierhorst, M. A. Wayne, M. J. Stevens, T. Gerrits, S. Glancy, D. R. Hamel, M. S. Allman, K. J. Coakley, S. D. Dyer, C. Hodge, A. E. Lita, V. B. Verma, C. Lambrocco, E. Tortorici, A. L. Migdall, Y. Zhang, D. R. Kumor, W. H. Farr, F. Marsili, M. D. Shaw, J. A. Stern, C. Abellán, W. Amaya, V. Pruneri, T. Jennewein, M. W. Mitchell, P. G. Kwiat, J. C. Bienfang, R. P. Mirin, E. Knill, and S. W. Nam, "Strong loophole-free test of local realism," Phys. Rev. Lett. **115**, 250402 (2015).

[10]H.-L. Yin, T.-Y. Chen, Z.-W. Yu, H. Liu, L.-X. You, Y.-H. Zhou, S.-J. Chen, Y. Mao, M.-Q. Huang, W.-J. Zhang, H. Chen, M. J. Li, D. Nolan, F. Zhou X. Jiang, Z. Wang, Q. Zhang, X.-B. Wang, and J.-W. Pan, "Measurement-device-independent quantum key distribution over a 404 km optical fiber," Phys. Rev. Lett. **117**, 190501 (2016).

[11]M. E. Grein, A. J. Kerman, E. A. Dauler, M. M. Willis, B. Romkey, R. J. Molnar, B. S. Robinson, D. V. Murphy, and D. M. Boroson, "An optical receiver for the lunar laser communication demonstration based on photon-counting superconducting nanowires," in *Advanced Photon Counting Techniques IX* (International Society for Optics and Photonics, 2015), Vol. 9492, p. 949208.

[12]S. Miki, M. Yabuno, T. Yamashita, and H. Terai, "Stable, high-performance operation of a fiber-coupled superconducting nanowire avalanche photon detector," Opt. Express. **25**, 6796–6804 (2017).

[13]A. J. Kerman, E. A. Dauler, W. E. Keicher, J. K. W. Yang, K. K. Berggren, G. Gol'tsman, and B. Voronov, "Kinetic-inductance-limited reset time of superconducting nanowire photon counters," Appl. Phys. Lett. **88**, 111116 (2006).

[14]J. Riu, M. Sicard, S. Royo, and A. Comerón, "Silicon photomultiplier detector for atmospheric lidar applications," Opt. Lett. **37**, 1229–1231 (2012).

[15]R. A. Barton-Grimley, R. A. Stillwell, and J. P. Thayer, "High resolution photon time-tagging lidar for atmospheric point cloud generation," Opt. Express **26**, 26030–26044 (2018).

[16]S. Isbaner, N. Karedla, D. Ruhlandt, S. C. Stein, A. Chizhik, I. Gregor, and J. Enderlein, "Dead-time correction of fluorescence lifetime measurements and fluorescence lifetime imaging," Opt. Express **24**, 9429–9445 (2016).

[17]J. Yang, A. Kerman, E. Dauler, V. Anant, K. Rosfjord, and K. Berggren, "Modeling the electrical and thermal response of superconducting nanowire single-photon detectors," Appl. Superconductivity, IEEE Trans. **17**, 581–585 (2007).

[18]M. Caloz, B. Korzh, N. Timoney, M. Weiss, S. Gariglio, R. J. Warburton, C. Schönenberger, J. Renema, H. Zbinden, and F. Bussières, "Optically probing the detection mechanism in a molybdenum silicide superconducting nanowire single-photon detector," Appl. Phys. Lett. **110**, 083106 (2017).

[19]F. Marsili, M. J. Stevens, A. Kozorezov, V. B. Verma, C. Lambert, J. A. Stern, R. D. Horansky, S. Dyer, S. Duff, D. P. Pappas, A. E. Lita, M. D. Shaw, R. P. Mirin, and S. W. Nam, "Hotspot relaxation dynamics in a current-carrying superconductor," Phys. Rev. B **93**, 094518 (2016).

[20]L. Zhang, L. You, X. Yang, J. Wu, C. Lv, Q. Guo, W. Zhang, H. Li, W. Peng, Z. Wang, and X. Xie, "Hotspot relaxation time of NbN superconducting nanowire single-photon detectors on various substrates," Sci. Rep. **8**, 1468 (2018).